Table 1. Atmospheric features probably attributable to current activity.

Feature	From latitude	Longitude	To latitude	Longitude
West plume	−49°	2°	−49°	352°
East plume	−57°	41°	−56°	27°
East plume companion 1	−59°	43°	−59°	36°
East plume companion 2	−60°	44°	−60°	37°
Limb haze with overshoot	−62°	67°	−69°	37°
Terminator cloud (fixed)	−37°	313°	−30°	337°
Crescent streak 1	−40°	144°	−40°	152°
Crescent streak 2	−41°	144°	−42°	152°
Crescent streak 3	−43°	133°	−44°	148°
Crescent streak 4	−47°	159°	−47°	170°
Crescent streak 5	−49°	154°	−49°	159°
Crescent streak 6	−51°	156°	−52°	167°

mal wind equation, the atmosphere over the equator must be warmer than that over the southern pole.

The surface stress in a laminar Ekman layer is exactly 45° to the left of the geostrophic wind (45° clockwise from north). The surface stress in a turbulent Ekman layer is closer to the direction of the geostrophic wind (*5*). One interpretation of our result, that the streaks are oriented predominantly 40° to 80° clockwise from north, is that the Ekman layer is turbulent. This interpretation is consistent with Ingersoll (*5*), who estimates that the eddy viscosity K is about 10 m^2 s^{-1}, several hundred times the molecular viscosity. Another interpretation is that the streaks are controlled by the wind slightly above the surface in a laminar Ekman layer. In this case streak orientation may be used to derive the material's altitude.

A major unknown is the thermal stratification of the atmosphere. If further analysis of the Voyager radio science, infrared, and ultraviolet spectrometer data were to give an improved temperature profile, then the level of turbulence and altitude of the streak material could be inferred from our data.

The latitudinal distribution of aeolian features is important evidence that plume activity is controlled by the seasonal migration of the subsolar latitude on Triton. Triton's subsolar latitude in 1989 was −45° while 10 years ago it was −35°. Maximum diurnal insolation occurs at the south pole, but subsurface temperatures may lag behind surface temperatures. This evidence, presented in more complete form here than elsewhere, is the basis for the assumption that the plumes are powered by solar energy. One possible explanation is that they are at least partially driven by greenhouse nitrogen (*7, 11*). Table 1 lists atmospheric features which are probably due to current eruptive activity. If this is the case, at least 12 eruptions are occurring on Triton simultaneously.

REFERENCES AND NOTES

1. B. Smith *et al.*, *Science* **246**, 1422 (1989).
2. L. Broadfoot *et al.*, *ibid.*, p. 1459.
3. G. Tyler *et al.*, *ibid.*, p. 1466.
4. B. Conrath *et al.*, *ibid.*, p. 1454.
5. A. Ingersoll, *Nature* **344**, 315 (1990).
6. B. Smith *et al.*, *Space Sci. Rev.* **21**, 103 (1977).
7. L. Soderblom *et al.*, *Science* **250**, 410 (1990).
8. C. Sagan, *Nature* **346**, 546 (1990).
9. A. McEwen *et al.*, *Geophys. Res. Lett.* **17**, 1765 (1990).
10. The locations and orientations of all aeolian features were measured using raw images and both VICAR and PICS image processing software. A cursor was placed at the source and termination of all wind streaks, plumes, and so on, and line and sample of the cursor was retrieved. Lines and samples of points measured were converted to latitude and longitude on a 1350-km radius Triton using the NAIF (Navigation Ancillary Information Facility at JPL) OLSEDR (Online Supplementary Experiment Data Record) program. From latitude and longitude both length and direction may be computed. A total of 132 features have been measured.
11. R. Brown *et al.*, *Science* **250**, 431 (1990).

12. This research was carried out by the Jet Propulsion Laboratory, California Institute of Technology, under a contract with the National Aeronautics and Space Administration. The authors thank the Voyager Flight Team for their careful implementation of a complicated imaging observation.

9 August 1990; accepted 24 September 1990

Subsurface Energy Storage and Transport for Solar-Powered Geysers on Triton

RANDOLPH L. KIRK, ROBERT H. BROWN, LAURENCE A. SODERBLOM

The location of active geyser-like eruptions and related features close to the current subsolar latitude on Triton suggests a solar energy source for these phenomena. Solid-state greenhouse calculations have shown that sunlight can generate substantially elevated subsurface temperatures. A variety of models for the storage of solar energy in a sub-greenhouse layer and for the supply of gas and energy to a geyser are examined. "Leaky greenhouse" models with only vertical gas transport are inconsistent with the observed upper limit on geyser radius of ~1.5 kilometers. However, lateral transport of energy by gas flow in a porous N_2 layer with a block size on the order of a meter can supply the required amount of gas to a source region ~1 kilometer in radius. The decline of gas output to steady state may occur over a period comparable with the inferred active geyser lifetime of five Earth years. The required subsurface permeability may be maintained by thermal fracturing of the residual N_2 polar cap. A lower limit on geyser source radius of ~50 to 100 meters predicted by a theory of negatively buoyant jets is not readily attained.

A HIGHLIGHT OF THE VOYAGER 2 encounter with Triton was the discovery of geyser-like plumes in the atmosphere, along with clouds and surface deposits (streaks) that may be related to the plumes in origin (*1–3*). The proximity of these features to the current subsolar latitude prompted the suggestion that the plumes are powered (or at least in some way triggered) by insolation. Smith *et al.* (*1*) outlined an insolation-driven geyser model in which sunlight is absorbed at the base of a "solid-state greenhouse" layer of clear nitrogen ice, increasing the subsurface temperature and creating a reservoir of high-pressure gas to feed the geyser in the pore space beneath. Subsequent calculations by Brown *et al.* (*4*) have confirmed that temperatures substantially (degrees or even tens of degrees) above ambient can be generated either in a thin, transparent "super greenhouse" layer underlain by a dark absorber or in a deeper, translucent "classical greenhouse."

The purpose of this report is to explore a range of models of the subsurface "plumbing" of an insolation-driven geyser: the processes by which absorbed solar energy is stored, transmitted, and released to supply nitrogen gas to the plume. Focusing on subsurface processes, we treat both the greenhouse layer and the erupting plume approximately, as simplified boundary conditions, rather than model them in detail. We attempt to construct models that can account for the observed and deduced properties of the geysers and to answer some of

the following questions: Are there any viable models, or do considerations of subsurface energy storage and transmission invalidate the solar geyser hypothesis? If viable models exist, do they involve a prolonged "charging" phase followed by a shorter period of "discharging," or is eruption close to equilibrium with energy input? Is lateral transport of energy or material important? How important is gas flow in transporting energy, compared with thermal conduction? What is the efficiency of the geyser mechanism, and what does it imply about the dimensions of the subsurface part of the geyser?

The most important of the geysers' properties constrained by the Voyager observations are their active lifetime, the quantity of gas erupted (hence the power required to drive the activity), and the size of the source region through which this gas passes. The preponderance of surface streaks over plumes active during the encounter (*3*) leads to a rough estimate for the geyser lifetime of one-tenth of a Tritonian season; in this report we use a value of five Earth years for the lifetime. Photometric analysis of the plume clouds (*2*) suggests that they entrain roughly 10 kg s^{-1} of dust, along with a slightly larger (but less certain) quantity of condensed N_2. The gas flux inferred from these observations is several hundred kilograms per second. We assume a nominal geyser power of 10^8 W, capable of subliming 400 kg of gas per second (*5*). The source radius may be as large as the observed ~1.5-km radius of the plumes (*2*), which indeed is suggested by moist-convective models of the plumes (*6*). Other models for the plumes are possible, however (*2*); an extreme case is the negatively buoyant jet model of Turner (*7*). In this model the source radius is determined by the volume and velocity of the erupted gas and is on the order of 50 to 100 m for thermal velocities corresponding to driving temperature differences of a few degrees (*8*).

Models that do not incorporate lateral energy transport generally fail to meet the above constraints, hence we describe only briefly two end members of this class. The first model is the "leaky greenhouse," in which the greenhouse layer is permeable and continually vents gas to the atmosphere. Even if as much as one-half of the flux $F_{sun} \simeq 0.85$ W m^2 (*9*) of absorbed sunlight could be used to vaporize gas (the remainder would be used to support the temperature gradient across the greenhouse layer), a minimum source radius of more than 8 km would be required for an output of 400 kg s^{-1}. The steady-state leaky greenhouse model also fails to account for the lifetime of the plumes, but a time-dependent variant is possible. We will return to it below in our discussion of time-dependent models with lateral transport. At the opposite extreme from the leaky greenhouse is the "champagne cork" model, motivated by the fact that the gas pressure at the base of a super greenhouse layer more than about 4 m thick can exceed that of the overburden (*4*). If the layer were completely impermeable, it might be explosively disrupted by the excess pressure. Gas would then be released to the atmosphere by evaporative cooling of the exposed hot ice, but activity would cease after the thermal-diffusion time for the largest fragments. This time is much less than a year even for meter-sized fragments, making the observation of active gas release during the Voyager encounter extremely unlikely in this model.

We instead consider models in which the geyser is supplied with energy from a larger, surrounding "collector" region. It is at once apparent that such a model will work only if energy is transported laterally by a mechanism more efficient than ordinary thermal conduction. The temperature differences driving lateral transport and upward heat loss through the greenhouse layer are similar in magnitude, but the horizontal distances are much larger. A larger effective conductivity is therefore required for lateral transport to be significant. This high effective conductivity must of course be prevented from operating in the greenhouse layer itself, or the upward heat flow will also be enhanced. We therefore restrict our attention to the super greenhouse model, in which the greenhouse effect takes place in a distinct thin layer. Any mechanism efficient enough to transport significant energy inward to the geyser will of course also transport energy outward, cooling the collector. Therefore, the greenhouse temperatures calculated by Brown *et al.* (*4*), who ignored lateral and downward energy loss, will be achieved only if the collector is made sufficiently large in relation to the greenhouse-layer thickness.

A candidate mechanism for enhanced energy transport is based on the strong temperature dependence of the equilibrium vapor pressure of nitrogen. Localized injection of heat will increase the pressure and drive gas flow through the pores toward cooler regions, where the gas will partly condense to maintain local equilibrium. Because of the latent heat of sublimation, energy as well as mass will be transported. This process is analogous to the operation of vapor-filled "heat pipes" used, among other purposes, for thermal control of spacecraft and for baking potatoes from the inside out.

We can quantify the effects of gas flow as follows. We begin by assuming local vapor-pressure equilibrium (*5*):

$$p \simeq p_\infty e^{-L/R^*T} \tag{1}$$

where L is the latent heat of sublimation, R^* is the universal gas constant divided by the molecular weight, and p_∞ is a constant. The assumption of equilibrium is justified because (as indicated above) the time scale for equilibration of solid nitrogen particles of any plausible size with the temperature of the surrounding gas is much less than a year. The gas density is given by the ideal gas law: $\rho = p/R^*T$. Next, we assume that gradients in pressure induce a flow of gas described by D'Arcy's law:

$$\mathbf{Q}_{mass} = -\frac{k_D \rho(T)}{\eta} \nabla p(T) \tag{2}$$

In this equation, $\mathbf{Q}_{mass}$ is the mass of gas passing through unit area of the porous medium in unit time, η is the viscosity of the gas and k_D is the D'Arcy permeability.

A net flux of gas into or out of a region will be accommodated by condensation or sublimation, respectively. The accompanying latent heat will appear in the equation of energy conservation for the medium:

$$\rho_s c_P (1 - \phi) \frac{\partial T}{\partial t} = k\nabla^2 T - L\left[\nabla \cdot \mathbf{Q}_{mass} + \phi \frac{\partial \rho(T)}{\partial t}\right] \tag{3}$$

where $\rho_s \simeq 990$ kg m^{-3} and $c_P \simeq 1340$ J kg^{-1} K^{-1} are the density and specific heat of the solid phase, $k \simeq 0.22$ W m^{-1} K^{-1} is its ordinary thermal conductivity (*10*), and ϕ is its porosity. Combining Eqs. 1, 2, and 3, we obtain the following equation for the temperature:

$$\left[(1 - \phi)\rho_s c_P + \phi\rho(T)\left(\frac{L}{R^*T^2} - \frac{1}{T}\right)\right]\frac{\partial T}{\partial t} = k\nabla^2 T + Lk_D \nabla \cdot \left[\frac{\rho(T)}{\eta(T)} \nabla p(T)\right] \tag{4}$$

This equation may be greatly simplified by ignoring all but the exponential dependences of pressure and density on temperature when taking the indicated derivatives. In this way we obtain

$$\frac{\partial T}{\partial t} \simeq \kappa \nabla^2 \Theta \tag{5a}$$

where

$$\Theta = T + \frac{Lk_D P(T)\rho(T)}{k\eta} \tag{5b}$$

This approximation includes the term modi-

R. L. Kirk and L. A. Soderblom, Branch of Astrogeology, U.S. Geological Survey, Flagstaff, AZ 86001.
R. H. Brown, Jet Propulsion Laboratory, California Institute of Technology, Pasadena, CA 91125.

fying the conductivity in Eq. 4 but not an analogous modification—negligible for the range of temperatures of interest—of the specific heat. The quantity Θ may be considered a "potential temperature," in that its gradient directly determines the heat flux: $\mathbf{F} = k\nabla\Theta$. We can also define an "effective conductivity" $k_{\text{eff}} = k\partial\Theta/\partial T$ [such that $\mathbf{F} = k_{\text{eff}}(T)\nabla T$], providing a convenient way of measuring the efficiency of energy transport. Using a simple model for the permeability as a function of porosity and block size (*11*), we find that for blocks a meter or more in diameter, the effective conductivity can be as much as 1000 times the ordinary thermal conductivity of N_2 (*10*) and ten times that of H_2O (*12*), at temperatures only a few degrees above the ambient temperature of roughly 38 K (*13*). Significant lateral energy transport is then possible over distances of kilometers, if the greenhouse layer thickness is of the order of meters. At the end of this paper we discuss the possibility that a layer of the required permeability is maintained by thermal fracturing.

The importance of gas in subsurface pores in the heat-pipe model is thus subtly different from that in the solar-geyser model as first proposed by Smith *et al.* (*1*): gas flow transports the energy to run the geyser, but the eruptive fluid is provided by evaporative cooling of warm N_2 solid; it is not stored in any significant quantity as gas in the pore spaces. The energy released by cooling a unit volume of solid by only 1 K is sufficient to produce roughly 40,000 volumes of gas at the ambient pressure.

Encouraged by the large effective conductivities possible for meter-sized blocks, we have undertaken numerical modeling of the region beneath a geyser and its solar collector. We begin by considering steady-state models. Not only are such models simpler to compute than time-dependent ones, but the results for a range of parameter values are more readily summarized. Study of the steady-state results is also helpful in understanding the time-dependent models presented below. Finally, there is the possibility that the subsurface gas flow is capable of persisting at the required volume for more than five Earth years and that some other process is responsible for shutting off the geysers. We will return to this possibility below.

In steady state, Eq. 5a for the potential temperature reduces to Poisson's equation, $\nabla^2\Theta = 0$. Realistic boundary conditions for a solar geyser are not so simple. On the solar collector we have a nonlinear, mixed boundary condition specifying that the upward conduction of heat through the greenhouse layer and the downward transport of gas must sum to the absorbed insolation. The "boundary condition" corresponding to the geyser is even more complicated: the gas supply from porous flow must match the output of the geyser, as must the temperature. Modeling the reservoir/geyser interface is beyond the scope of this paper. We instead approximate the geyser's effect on the subsurface by a region in which the temperature is held at the ambient value. A real geyser can extract no more energy from the system than such a cold patch without violating the second law of thermodynamics. On the collector (a larger surface region surrounding the source) we impose either fixed heat flux (Neumann) or fixed temperature (Dirichlet) boundary conditions. These conditions, respectively, are the appropriate limits of a realistic mixed boundary condition for small or large collectors, and they can be written purely in terms of the potential temperature or its gradient, leading to a linear problem to be solved for Θ (*14*).

The model geometry is axisymmetric, with the collector concentric to the geyser source area. There is some suggestion that the surface streaks on Triton preferentially originate from points on the edges of subcircular albedo markings on the south polar cap, but even if these markings represent the geyser collectors, the axisymmetric model captures the essential feature of convergent flow toward the geyser outlet. To achieve the steady-state solution, we used an explicit time-stepping finite-difference scheme (*15*) applied to the fictitious linear diffusion equation $\partial\Theta/\partial t = \nabla^2\Theta$. A multigridding scheme (*16*) was used to obtain convergence on grids as large as 513 by 513 in reasonable time, despite the small time steps required for stability.

The parameters defining the models are collector disk radius R_d, geyser source area radius R_g, permeable layer depth Z, grain diameter b, and either the heat flux F_{in} into a Neumann collector or the temperature on a Dirichlet collector. The output quantities of greatest interest are the peak temperature $T_{\max}$, corresponding to the enhancement of potential temperature by $\Delta\Theta_{\max}$ under a constant-flux collector, and the power P_{out} emerging from the geyser. These quantities are connected by simple scaling relations with numerical factors obtained from our models.

We find that for a constant-flux collector with no central geyser over a permeable layer with depth $Z \gtrsim R_d$,

$$\Delta\Theta_{\max} \simeq 0.29\ \frac{F_{\text{in}}R_d}{k} \qquad (6a)$$

while for $Z << R_d$ we obtain

$$\Delta\Theta_{\max} \simeq 0.09\ \frac{F_{\text{in}}R_d^2}{kZ} \qquad (6b)$$

The actual temperature corresponding to $\Delta\Theta_{\max}$ depends on the ambient temperature and permeability according to Eq. 5b. These relations were used previously (*17*) to obtain a crude estimate of the collector radius at which the subsurface temperature approaches the maximum attainable for a given greenhouse layer, by equating $\Theta_{\max}$ to the potential temperature corresponding to the greenhouse temperature and F_{in} to an arbitrary but small fraction of the input energy supply. In this paper, we use a slightly more realistic approximation to the radius dependence of temperature. Given a sub-greenhouse temperature $T_{\max} = T_0 + \Delta T$, we calculate $\Delta\Theta_{\max}$ from Eq. 5b, and in Eq. 6 we set F_{in} equal to the fraction of the absorbed insolation not lost through the greenhouse layer, that is, $F_{\text{in}} = F_{\text{sun}} - k\Delta T/Z_g$, where Z_g is the thickness of the greenhouse layer. We thereby reproduce the qualitative behavior of $T_{\max}(R_d)$, which is determined by a constant-flux model with input flux F_{sun} for small radii, but which is asymptotic to the maximum greenhouse temperature (*4*) for large radii. The solid curves in Fig. 1 illustrate this behavior for Z = 10 and 100 m and Z_g = 2 and 4 m (*18*) for a range of grain sizes b.

We next consider the power available to run the geyser (*19*). Fixed-temperature models give $P_{\text{out}} \propto k\Delta\Theta_{\max}R_g$, with proportionality constants of 14 and 9.8 for thick and thin models, respectively (*20*). For thick fixed-flux models we obtain $P_{\text{out}} = \pi R_g R_d F_{\text{in}}$, which, when combined with Eq. 6a, gives $P_{\text{out}} = 11k\Delta\Theta_{\max}$. Only the thin Neumann models depart from this scaling: $P_{\text{out}} = 2.5\pi R_g R_d F_{\text{in}}$ combined with Eq. 6a gives $P_{\text{out}} = 87k\Delta\Theta_{\max}R_gZ/R_d$. We are primarily interested in collectors that are close to the maximum greenhouse temperature (that is, closer to the fixed-temperature case), so we adopt the relation

$$P_{\text{out}} \simeq 10k\Delta\Theta_{\max}R_g \qquad (7)$$

to summarize our results. This equation is plotted for a range of grain sizes as the dashed curves in Fig. 1, assuming a power output $P_{\text{out}} = 10^8$ W as inferred above.

A trivial constraint on the models is $R_g < R_d$; as indicated above, $R_g < R_d/4$ is more reasonable if the peak sub-greenhouse temperature is not to be appreciably reduced by the geyser. These relations between the collector and geyser radii are indicated in Fig. 1 by the dash-dot curves. An upper limit of 400 to 800 m (for Z = 10 to 100 m) is evidently imposed on R_g unless the geyser operates near the maximum attainable temperature for a given greenhouse thickness (that is, unless only a small fraction of the absorbed solar energy is lost through the permeable layer). This limit is not ap-

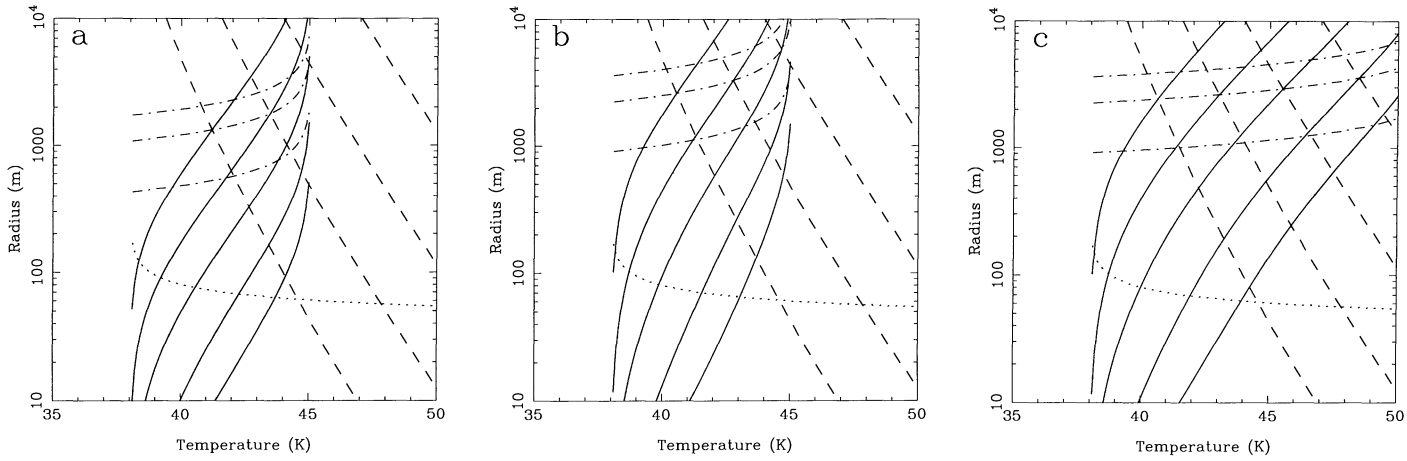

Fig. 1. Solid curves: solar-collector radius required to achieve a given maximum temperature. Dashed curves: geyser-source radius required to yield 10^8 W power output at given temperature for N_2 block sizes of 10 cm, 30 cm, 1 m, 3 m, and 10 m (right to left). Dash-dot curves: source radius equal to 1/4 collector radius, source radius equal to collector radius, and collector radius equal to four times source radius for given temperature and same block size. Dotted curve: minimum geyser radius required to deliver a gas flux of 400 kg s^{-1} at the thermal expansion velocity. Panels correspond to (**a**) greenhouse depth Z_g = 2 m and permeable layer depth Z = 10 m, (**b**) Z_g = 2 m and Z = 100 m, and (**c**) Z_g = 4 m and Z = 100 m.

proached by the minimum source size for a negatively buoyant plume, but if the source area has a diameter on the order of a kilometer, as in the models of Yelle *et al.* (*6*), or even 3 km, which is consistent with the Voyager images (*2*), then most of the energy is conducted to the surface and only a small fraction is channeled to the geyser. The collector radius may have any value above the minimum; the geyser temperature is determined by the greenhouse thickness (*4*), as illustrated in Fig. 2. This figure also shows the sub-greenhouse grain size b needed to channel 10^8 W to a geyser 1.5 km in radius and to the minimum size source for a negatively buoyant plume at the given temperature. The temperatures and grain sizes required for the smaller source are extreme and may not be attainable on Triton.

We have also modeled the time-dependent behavior of a newly opened geyser, with three major goals in mind. First, we would like to predict the lifetime of geyser activity as a consequence of the dynamics of subsurface energy transport. Second, we hope to relax the requirements for subsurface permeability imposed by the steady-state models. Finally, we are interested in determining the extent to which time dependence can reconcile the geyser source radius with the predictions of negatively buoyant jet theory.

We begin with a one-dimensional model in which a layer of depth Z, initially at temperature $T_0 + \Delta T$, has an upper boundary at temperature T_0 and an insulating lower boundary. The result is very similar to that for the analogous problem with linear thermal conduction: the heat flux declines as $t^{-1/2}$ until a time on the order of Z^2/κ (when the bottom of the layer has begun to cool significantly), then falls much more rapidly. The main difference is that the effective thermal diffusivity $\kappa_{eff} = k_{eff}/\rho c_p$ is a function of temperature. For temperature differences of a few degrees or more, we find that the change in cooling behavior occurs at a time $Z^2/\kappa_{eff}(T_0 + \Delta T)$, that is, it is the effective conductivity at the maximum temperature that determines the lifetime. In Fig. 3 we illustrate the diffusion length corresponding to a geyser lifetime of five Earth years as a function of temperature and grain size.

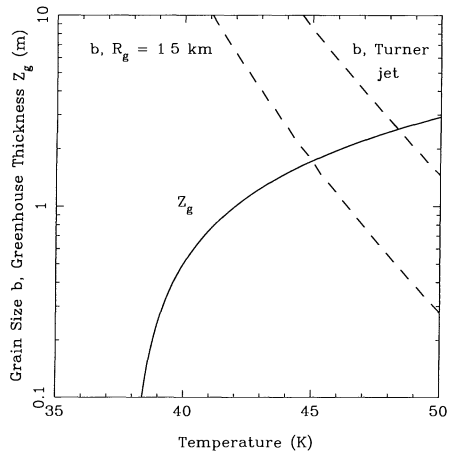

Fig. 2. Summary of steady-state solar geyser behavior. Solid curve: greenhouse layer thickness required for given temperature under a large collector. Dashed curves: sub-greenhouse block diameter required to delivery 5×10^6 W to geyser source with radius R_g = 1.5 km (left) and block diameter required for R_g predicted by negatively buoyant jet theory (right).

For a time-dependent deep geyser model, the results are almost equally straightforward. For simplicity we consider the inner portion of a Dirichlet collector, so that the initial condition before opening of the geyser is $T = T_0 + \Delta T$ everywhere, and after opening the geyser to $T = T_0$ we maintain this elevated temperature on the other boundaries; in this way we avoid having to calculate a complicated initial temperature distribution under the whole collector. In this model, the power declines approximately as $t^{-1/3}$ at first, then levels out at the steady-state power calculated above by the time $t \simeq R_g^2/\kappa_{eff}(T_0 + \Delta T)$. We expect that the early history of a "time-dependent leaky geyser" model (with no collector surrounding the newly opened geyser) would be similar, but that after $t \simeq R_g^2/\kappa_{eff}$ the power would tend rapidly to zero, rather than to a steady-state output.

Because of the nonlinear conduction mechanism, the thermal energy released by cooling is proportional to the logarithm of the collector-geyser temperature difference rather than to the temperature difference itself. For ΔT of a few degrees, we find that $\Delta E \simeq 1.5\ \mathrm{K} \cdot 2\pi/3\ R_g^3 \rho_s c_p$. It is thus not possible to construct a time-dependent model with $R_g \sim 50$ to 100 m, as predicted by the negatively buoyant jet model. To store the energy to run a geyser at 10^8 W for five Earth years we require $R_g \simeq 1.6$ km, virtually independent of the maximum temperature. The corresponding radius for a thin layer is even larger.

More realistic models in which a geyser opens into a thin permeable layer combine

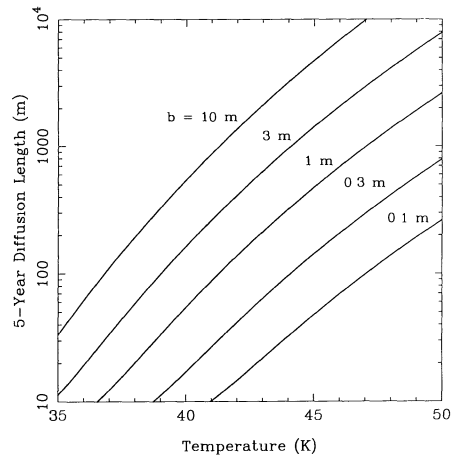

Fig. 3. Thermal-diffusion distance over a five-Earth-year period computed using the effective conductivity of porous N_2 with five block sizes of 10 cm, 30 cm, 1 m, 3 m, and 10 m.

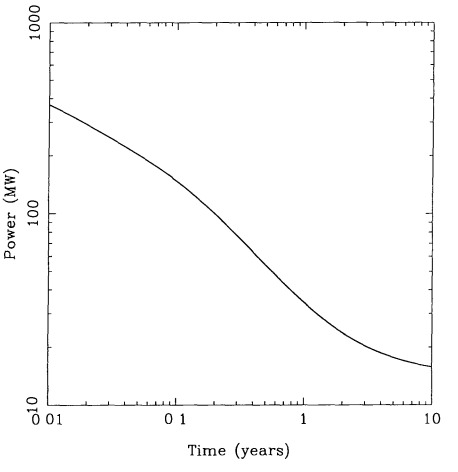

Fig. 4. Example of a time-dependent geyser model with greenhouse temperature of 44.5 K, subgreenhouse block diameter of b = 1 m, permeable layer depth Z = 100 m, and geyser source radius R_g = 1510 m. Diffusion time based on depth is 0.1 Earth years; based on radius and depth, 3.5 years.

aspects of the behavior of the above cases. The output power initially declines roughly as $t^{-1/3}$ until $t \simeq 0.4Z^2/\kappa_{eff}$, when the bottom center of the layer has started to cool. A steeper decline then ensues until the steady-state power is reached at $t \simeq 0.7\ R_dZ/\kappa_{eff}$. The parameter space for these shallow time-dependent models is obviously very large; we show in Fig. 4 one example that very roughly approximates the inferred behavior of the Tritonian geysers. With $T_0 + \Delta T$ = 44.5 K, b = 1 m, Z = 100 m, and R_g = 1510 m (*21*), the depth time scale is 0.1 year and the radius time scale is 3.5 years. The power declines from over 10^8 W in the first 3 months to a steady-state value of 1.5×10^7 W. As this example shows, the intrinsic time dependence of flow from a newly tapped greenhouse layer may explain the inferred lifetime of Triton's geysers, but it is too weak to reduce the required permeability appreciably compared with the steady-state models. The eruption rate exceeds its steady-state value by a factor of 10 (allowing a threefold reduction in grain size) only for a small fraction of the time required to reach steady state.

The calculations presented here lend credibility to the idea that Triton's geysers are solar powered. At temperatures only a few degrees above the planetary average, flow in subsurface pores can supply hundreds of kilograms of gas per second to a geyser source area several hundred meters to a few kilometers in radius. Despite the efficiency of this gas flow in transporting energy, the temperatures calculated for a solid-state greenhouse layer of infinite lateral extent (*4*) can be approached in a "solar collector" only a few times larger than the geyser. The vigorous initial release of gas that follows opening of a geyser vent in such a collector lasts on the order of a few Earth years for plausible choices of the system dimensions. The length of this period of enhanced gas flow may account for Voyager 2 having observed roughly ten surface streaks for every currently active geyser, although other explanations are possible. One alternative is that the geyser chokes on its own dust. If only one part in 10^4 of the estimated 10 kg of dust per second emitted by a geyser falls back onto a solar collector 3 km in radius, the collector will be buried at a rate of roughly 1 μm per year. Sunlight will increasingly be absorbed by this surface dust rather than by the base of the greenhouse layer, which will effectively shut off the energy supply for the geyser after a few years.

To obtain lateral gas transport of the stated magnitude, we require a very high D'Arcy permeability, $k_D \simeq 10^{-7}$ to 10^{-3} m^2, depending on the temperature, in a subsurface layer perhaps 10 to 100 m thick. This layer must be capped by a greenhouse layer a few meters thick whose permeability is much less. The required permeability is far in excess of the values reported for fractured terrestrial lava (*22*), but it is only slightly beyond the range of values commonly tabulated for sediments (*11*). The existence of such a permeable subsurface layer on Triton must be considered highly speculative, but we believe that thermal stresses may provide a mechanism for creating and maintaining such a layer. The thermal expansivity of solid nitrogen is large, $\sim 2.5 \times 10^{-3}$ K^{-1} (*10*), and in addition, a volume change of the order of 1% accompanies the α-β phase transition. This volume change reportedly often disrupts nitrogen samples undergoing the phase transition in the laboratory (*10*). Annual temperature fluctuations in the subgreenhouse layer could thus engender volume changes of several percent, especially if the minimum temperature were within the stability field of the α phase. The transition temperature lies within the formal uncertainty of Voyager estimates of the surface temperature of Triton (*13*) for pure N_2 and may be increased by as much as several degrees if CO is present in the polar caps in solid solution (*10*). Thermal fracturing and jostling of the fragments could thus produce substantial porosity in the layer. If the fracture spacing were controlled in part by the thickness of the nitrogen layer, the meter-sized "grains" posited would not be unreasonable for a layer some meters thick. Alternatively, the gas may flow through a few large fissues of tectonic origin, rather than through a multitude of smaller pores.

The permeability and fragility of the greenhouse layer also have a major effect on the expected size and behavior of the geysers. If the layer is for the most part permeable, the "leaky geyser" model will apply, with gas transport primarily vertical; such a model is unattractive because the source region must be larger than about 8 km in radius. On the other hand, how could an impermeable layer be created and maintained on top of the fractured deep layer, and what processes are responsible for breaching it locally to create a geyser source area? Are localized areas highly permeable from the start, so that gas escapes in steady state as the greenhouse warms up in spring? Or does some process—for example, thermal erosion—open a path for gas once the subsurface temperature is high? Do these processes operate only rarely, so that $R_g << R_d$ (as is required if the source is as small as the negatively buoyant jet model predicts), or are they more common, so that $R_g \lesssim R_d$? We do not have the answers to these questions, but we offer one speculation on the creation of a mostly impermeable greenhouse layer. This layer may be the seasonal N_2 deposit, and hence it would be reconstituted each Tritonian year. Solid-state diffusion calculations (*23*) suggest that grain growth by annealing over a Tritonian year will not yield nitrogen crystals of sufficient size to account for the observed 2.15 μm absorption in Triton's disk-averaged spectrum (*24*). The ease with which centimeter-sized crystals of nitrogen can be grown from vapor in the laboratory (*10*) prompts us to wonder whether the seasonal layer on Triton comprises massive, vapor-deposited crystals rather than frost. Such crystals might account not only for the large optical path lengths inferred for most of Triton's surface, but also for the ability of an even more transparent greenhouse layer present in restricted areas to seal off the subsurface pore space.

REFERENCES AND NOTES

1. B. A. Smith *et al.*, *Science* **246**, 1422 (1989).
2. L. A. Soderblom *et al.*, *ibid.* **250**, 410 (1990).
3. C. Hansen *et al.*, *ibid.*, p. 421.
4. R. H. Brown *et al.*, *ibid.*, p. 431.
5. A fit to vapor-pressure [in R. C. Weast, Ed., *Handbook of Chemistry and Physics* (CRC Press, Cleveland, ed. 56, 1975), p. D186] gives $p_\infty = 7.9 \times 10^9$ Pa, $L = 2.5 \times 10^5$ J kg^{-1} K^{-1} in Eq. 1.
6. R. V. Yelle *et al.*, in preparation.
7. J. S. Turner, *J. Fluid Mech.* **26**, 779 (1966).
8. S. W. Kieffer, in *Satellites of Jupiter*, D. Morrison, Ed. (Univ. of Ariz. Press, Tucson, 1982), pp. 647–723.
9. Because the thermal-diffusion time for a layer a few meters thick is on the order of months to years, we consider the diurnally averaged solar energy input $F_{sun} = [L_s (1 - A)/4\pi R^2]\bar{\alpha}$, where $L_s = 3.83 \times 10^{28}$ W is the bolometric luminosity of the sun, $R = 4.52 \times 10^{12}$ m is the heliocentric distance of Triton, A is the albedo of the absorbing layer below the greenhouse (taken as 0.05), and $\bar{\alpha}$ is the diurnal average of the cosine of the incidence angle. We use $\bar{\alpha} = 0.6$, appropriate to a subsolar latitude of 45°S and a latitude intermediate between the two active plumes.
10. T. A. Scott, *Phys. Rep.* **27**, 3 (1976).
11. D. L. Turcotte and G. Schubert, *Geodynamics* (Wiley, New York, 1982), pp. 381–384. We use a constant permeability of 0.1 in our models. The mass of gas erupted over five Earth years is typically on the order of a percent of the mass of the sub-greenhouse layer, so that we do not expect substantial changes in the mean porosity. Thermal erosion may, however, result in some enhancement of the permeability near the geyser, where the net cooling for a time-dependent model is greatest.
12. N. H. Fletcher, *The Chemical Physics of Ice* (Cambridge Univ. Press, Cambridge, 1970), pp. 143–146.
13. B. Conrath *et al.*, *Science* **246**, 1454 (1989), A. L. Broadfoot *et al.*, *ibid.*, p. 1459.
14. The boundary conditions imposed at depth and at the outer edge of the modeled region also affect the linearity of the problem. Constant potential temperature was imposed on both to model a deep geyser, while for a shallow geyser the outside edges were held at constant temperature but the bottom boundary was made insulating. The latter is an adequate approximation even if an H_2O-ice layer underlies the permeable layer, because the posited effective conductivity is roughly ten times that of ice.
15. W. H. Press *et al.*, *Numerical Recipes* (Oxford Univ. Press, Oxford, 1986), pp. 635–640.
16. A. Brandt, *Math. Comp.* **31**, 331 (1974).
17. R. L. Kirk, *Lunar Planet. Science* **21**, 663 (1990).
18. The distribution of temperatures under the actual collector will of course depart from the Neumann model as R_d increases. With constant flux, the model predicts decreasing temperatures toward the edges of the collector; in reality a decreased sub-greenhouse temperature leads to an increased downward heat flux. The actual temperature distribution will thus be intermediate between the Neumann and Dirichlet models, but the central temperature should be close to that predicted here. We have also calculated curves for a deep layer ($Z >> R_d$) but do not present them because viscous-relaxation calculations [R. L. Kirk, *Lunar Planet. Science* **21**, 635 (1990)] suggest that the global N_2 layer on Triton is no more than 30 to 100 m thick. A thick layer of high effective conductivity cannot be ruled out entirely, however, because the heat-pipe mechanism could operate in permeable H_2O-ice if the pore surfaces were encrusted with solid nitrogen. A further consideration is that the time required to warm a deep layer may exceed the length of the Tritonian summer. This is not necessarily a fatal objection, because condensation on the surface will prevent winter cooling from offsetting summer warming—provided gas flow cannot carry energy away from the subsurface layer—but localized eruption in the northern (winter) hemisphere would be as likely as eruption in the southern hemisphere in such a model. Curves for $Z_g = 1$ m are omitted here as well. They qualitatively resemble those for thicker greenhouse layers, but the limiting temperature is only about 42 K.
19. The power delivered to the geyser consists of insolation onto the source area (proportional to R_g^2) and the contribution from the collector (proportional to $R_g R_d$). The latter thus dominates for $R_g << R_d$, and because we find that $R_g \leq R_d/4$ is required for the peak temperatures of Eq. 6 to apply, we neglect the contribution of insolation onto the geyser.
20. The abrupt transition between $T = T_0$ on the geyser and $T = T_0 + \Delta T$ on the collector in the Dirichlet models leads to a $1/(R - R_g)$ divergence of the flux near the boundary, and hence a logarithmic dependence of P_{out} on the mesh spacing. In reality, the limit on available flux will lead to a temperature transition over a small but finite zone even if the inner edge of the greenhouse collector is perfectly sharp. The coefficients given in the text are for $R_g = 128$ mesh steps.
21. The calculation was carried out on a 5 by 257 mesh, with a mesh spacing of 20 m and R_g halfway between nodes at 75.5 steps from the axis. From the results for steady-state models, $R_g \simeq 1.5$ km implies $R_d \geq 6$ km, and hence a collector operating near its maximum greenhouse temperature. We then find $Z_g \simeq 2$ m to achieve a temperature of 44.5 K.
22. M. H. Carr, *J. Geophys. Res.* **84**, 2995 (1979).
23. R. L. Kirk, *Lunar Planet. Sci.* **21**, 635 (1990).
24. D. P. Cruikshank, R. H. Brown, R. N. Clark, *Icarus* **58**, 293 (1984).

9 August 1990; accepted 26 September 1990

Temperature and Thermal Emissivity of the Surface of Neptune's Satellite Triton

ROBERT M. NELSON, WILLIAM D. SMYTHE, BRAD D. WALLIS, LINDA J. HORN, ARTHUR L. LANE, MARVIN J. MAYO

Analysis of the preliminary results from the Voyager mission to the Neptune system has provided the scientific community with several methods by which the temperature of Neptune's satellite Triton may be determined. If the 37.5 K surface temperature reported by several Voyager investigations is correct, then the photometry reported by the imaging experiment on Voyager requires that Triton's surface have a remarkably low emissivity. Such a low emissivity is not required in order to explain the photometry from the photopolarimeter experiment on Voyager. A low emissivity would be inconsistent with Triton having a rough surface at the ~100-μm scale as might be expected given the active renewal processes which appear to dominate Triton's surface.

SURFACE TEMPERATURE IS ONE OF several important factors that constrain models of the physical and chemical processes occurring on an object in the solar system. For this reason, several Voyager experiments endeavored to measure parameters from which the temperature of Triton could be determined. Triton's surface temperature has been derived or inferred by at least five separate Voyager investigations.

One technique is to develop a model atmospheric thermal profile and extrapolate it to Triton's surface. This method was employed by the investigators on the ultraviolet spectrometer (UVS) experiment (*1*). Their atmospheric model thermal profile, extrapolated to Triton's surface, was consistent with a surface pressure of 14 μbar. This is the equilibrium vapor pressure of nitrogen, a proposed dominant atmospheric gas, at 37.5 K. Likewise, the atmospheric occultation experiment conducted by the radio science (RSS) team investigators is consistent with the equilibrium atmosphere pressure derived by UVS if a model is fit which assumes an inversion layer in Triton's atmosphere at a height of 5 km above the surface (*2*).

A direct method of determining the temperature of Triton's surface is to measure the thermal radiation emitted at infrared wavelengths. The Voyager Infrared Interferometer Spectrometer and Radiometer (IRIS) measured the infrared radiation emitted from Triton's surface. The IRIS investigators averaged 16 infrared spectra from Triton's dayside and their best fit to the data yielded a temperature of 38 K, assuming that Triton radiates like a blackbody (for which emissivity = 1.0). They estimated the error in their measurement by deriving the temperatures expected by adding an additional 5% to the RMS residual of the fits. This is considered to be a conservative, subjective estimate of the 2 σ errors (*3*) and yields a temperature of 38^{+3}_{-4} K. They also fit a model to the IRIS data which assumed an emissivity of 0.5 which resulted in a temperature of 41^{+3}_{-5} K. This result is somewhat higher but has an error large enough to be consistent with the UVS result (*4*).

Photometric data have also been employed for determining Triton's surface temperature (*5*). This requires calculation of Triton's bolometric Bond albedo (the ratio of the integrated energy flux over all wavelengths from Triton in all directions to the solar insolation). Estimation of the bolometric Bond albedo permits derivation of an average temperature assuming thermal equilibrium.

Jet Propulsion Laboratory, Pasadena, CA 91109.